Gray, White Matter Concentration Changes and Their Correlation with Heterotopic Neurons in Temporal Lobe Epilepsy

Woo Suk Tae, PhD[1, 3]
Eun Yun Joo, MD[1]
Sung Tae Kim, MD[2]
Seung Bong Hong, MD[1]

Index terms:
Temporal lobe epilepsy
Magnetic resonance (MR)
Heterotopic neuron
Voxel-based morphometry
Gray matter concentration
White matter concentration

DOI:10.3348/kjr.2010.11.1.25

Korean J Radiol 2010;11:25-36
Received January 27, 2009; accepted after revision August 27, 2009.

Departments of Neurology[1] and Radiology[2], Samsung Medical Center, Sungkyunkwan University School of Medicine, Seoul 135-710, Korea; Neuroscience Research Institute[3], Kangwon National University School of Medicine Kangwon-do 200-701, Korea

This study was supported by a Grant (2009K001257) from the Brain Research Center of the 21st Century Frontier Research Program, which was funded by a Ministry of Science, by the Samsung Biomedical Research Institute grant, #SBRI C-A7-226-3, and partly by a Korea Research Foundation Grant funded by the Korean Government [KRF-2008-359-E00009]

Address reprint requests to:
Seung Bong Hong, MD, Department of Neurology, Epilepsy Center, Samsung Medical Center, Sungkyunkwan University School of Medicine, 50 Ilwon-dong, Gangnam-gu, Seoul 135-710, Korea.
Tel. (822) 3410-3592
Fax. (822) 3410-0052
e-mail: sbhong@skku.edu, sbhongsmc@gmail.com

Objective: To identify changes in gray and white matter concentrations (GMC, WMC), and their relation to heterotopic neuron numbers in mesial temporal lobe epilepsy (mTLE).

Materials and Methods: The gray matter or white matter concentrations of 16 left and 15 right mTLE patients who achieved an excellent surgical outcome were compared with those of 24 healthy volunteers for the left group and with 23 healthy volunteers for the right group, by optimized voxel-based morphometry using unmodulated and modulated images. A histologic count of heterotopic neurons was obtained in the white matter of the anterior temporal lobe originating from the patients' surgical specimens. In addition, the number of heterotopic neurons were tested to determine if there was a correlation with the GMC or WMC.

Results: The GMCs of the left and right mTLE groups were reduced in the ipsilateral hippocampi, bilateral thalami, precentral gyri, and in the cerebellum. The WMCs were reduced in the ipsilateral white matter of the anterior temporal lobe, bilateral parahippocampal gyri, and internal capsules, but increased in the pons and bilateral precentral gyri. The heterotopic neuron counts in the left mTLE group showed a positive correlation ($r = 0.819$, $p < 0.0001$) with GMCs and a negative correlation ($r = -0.839$, $p < 0.0001$) with WMCs in the white matter of the anterior temporal lobe.

Conclusion: The present study shows the abnormalities of the cortico-thalamo-hippocampal network including a gray matter volume reduction in the anterior frontal lobes and an abnormality of brain tissue concentration in the pontine area. Furthermore, heterotopic neuron numbers were significantly correlated with GMC or WMC in the left white matter of anterior temporal lobe.

Mesial temporal lobe epilepsy (mTLE) is the most common type of intractable partial epilepsy, and hippocampal sclerosis is the most frequent pathological finding in mTLE (3). Brain MRI has been successfully used for detecting epileptogenic lesion (4). Hippocampal sclerosis is easily visible on MR images, but it is difficult to detect mild structural abnormalities in other brain structures of mTLE patients. A voxel-based morphometry (VBH) provides a quantitative means of examining brain MR images in terms of structural differences or for performing statistical analysis, and has been widely used to detect subtle changes of the brain structures in the cerebral cortex, limbic structures, subcortical nuclei (2, 3), and cerebral white matter (1, 5) of mTLE patients. A previous study was conducted to identify correlations between gray matter concentrations (GMCs) and hippocampal volumes (6).

In VBM, the GMCs generally reflect the amount of neuronal concentration, whereas

white matter concentrations (WMCs) indicate the amount of nerve fibers or myelinated axons. Past reports have described the presence of heterotopic neurons in the anterior temporal stem of mTLE patients (7, 8). In addition, the relationship between heterotopic neurons of the anterior temporal stem and the ictal hyperperfusion was previously suggested (9). From these observations, we speculated that a correlation exists between the GMCs and the heterotopic neuron counts in the white matter of the anterior temporal lobe.

The aim of the present study was to investigate structural changes in pathologically proven unilateral mTLE patients using optimized VBM, as well as determine whether a correlation exists between heterotopic neuron counts for the gray and WMCs.

MATERIALS AND METHODS

Patients

We included 31 unilateral mTLE patients (16 left [5 men, 11 women] and 15 right [7 men, 8 women]) who achieved excellent surgical outcomes (Engel class I) after an anterior temporal lobectomy with amygdalohippocampectomy (Table 1). To include only patients whose seizures arise from the mesial temporal lobe, we excluded patients who did not have a postoperative seizure-free outcome because they may have had a seizure focus in another region such as the lateral temporal cortex or extratemporal regions. Hippocampal sclerosis was pathologically confirmed in all cases. The clinical characteristics collated for each subject were at the age of seizure onset, duration of epilepsy, white matter changes of the anterior temporal lobe (WCAT), as well as though the number of heterotopic neurons by MRI and by the pathology. The data of all patients were collected at the Samsung Medical Center from 2004 to 2006.

For comparative purposes twenty four healthy volunteers (8 men, 16 women) made up the left mTLE group, while 23 healthy volunteers (12 men, 11 women) made up the right mTLE group (Table 1). Because the age and sex distributions of the left and right mTLE groups were different, two cohorts of normal controls were prepared to match the respective age and sex distribution. These healthy subjects had no history of head trauma or of a neurological or psychiatric disorder and were not on a medication. Moreover, the healthy subjects all had a normal spoiled gradient recalled in the steady state (SPGR) MRI findings, and showed no signal changes in the fluid attenuated inversion recovery (FLAIR) or T2-weighted images.

Abbreviations:
CSF = cerebrospinal fluid
DTI = diffusion tensor imaging
FA = fractional anisotropy
FDR = false discovery rate
FLAIR = fluid attenuated inversion recovery
FOV = field of view
FWE = family-wise error
FWHM = full-width at half maximum
GM = gray matter
GMC = gray matter concentration
MNI = Montreal Neurological Institute
mTLE = mesial temporal lobe epilepsy
NEX = number of excitations
rCBF = regional cerebral blood flow
SPGR = spoiled gradient recalled
SPM = statistical parametric mapping
VBM = voxel-based morphometry
WCAT = white matter changes of the anterior temporal lobe
WM = white matter
WMAT = white matter of anterior temporal lobe
WMC = white matter concentration
WMV = white matter volume

Magnetic Resonance Imaging

MRI scanning was performed using a GE Signa 1.5 Tesla scanner (GE Medical Systems, Milwaukee, WI). All subjects underwent SPGR, T2-weighted, and FLAIR imaging protocols. Coronal SPGR MR images were obtained using the following scanning variables; 1.6 mm thickness, no gap, 124 slices, repetition time/echo time (TR/TE) = 30/7 milliseconds (msec), flip angle (FA) = 45°, number of excitations (NEX) = 1, matrix = 256 × 192, and field of view (FOV) = 22 × 22 centimeters (cm). The voxel dimension of the SPGR MR images was 0.86 × 0.86 × 1.6 mm. An oblique coronal FLAIR MRI was performed using a 4.0 mm slice thickness, 1.0 mm gap, 32 slices, TR/TE = 10002/127.5 msec, 1 NEX, matrix = 256 × 192, and a FOV = 20 × 20 cm. The oblique coronal T2-weighted MR images were obtained with a 3.0 mm slice thickness, 0.3 mm gap, 56 slices, TR/TE = 5300/99 msec, FA = 90°, 3 NEX, matrix = 256 × 192, and FOV = 20 × 20 cm.

Voxel-Based Morphometry

Using SPM2 (Wellcome Department of Cognitive Neurology, Institute of Neurology, University College London) and MATLAB 7.0 (The MathWorks, Natick, MA), an optimized VBM protocol (9) was performed to determine GMCs and WMCs and regional volume changes. To create customized templates and prior images of gray and white matter, all MR images from the mTLE patients and normal controls were spatially normalized to a standard T1 template. Spatial normalizations were applied using the following parameters: voxel size = 1 × 1 × 1 mm, cutoff spatial normalization of 25 mm, nonlinear regularization = medium, and 16 nonlinear iterations. The normalized images were segmented into gray matter, white matter, cerebrospinal fluid (CSF), and sub-sampled

into a voxel size of $2 \times 2 \times 2$ mm. The spatially normalized raw images, segmented gray matter, white matter, and CSF images were averaged and saved into the customized T1 template, gray matter, white matter, or CSF prior images, respectively. Finally, three previously obtained images and the customized T1 template were smoothed using an 8 mm full-width at half-maximum (FWHM) isotropic Gaussian kernel. The raw T1 images of all subjects were automatically segmented into gray matter, white matter, and CSF partitions in native space, and volumes of gray and white matter images were then calculated. The spatial normalization parameters were estimated by matching each individual's own gray matter with SPM to the gray matter template of this study, to create spatially normalized versions of the original images. Spatially normalized images were segmented using each patients' own prior images (gray matter, white matter, and CSF partitions), and then spatially normalized. Moreover, the segmented gray and white matter images were modulated for regional volume change analyses. Modulated images were smoothed using an 8 mm FWHM isotropic Gaussian kernel, whereas unmodulated images were smoothed using a 12 mm FWHM isotropic Gaussian kernel. An unmodulated VBM is indicative of concentration differences, whereas modulated VBM is indicative of volume differences.

Neuronal Counting and Criteria for White Matter Changes of Anterior Temporal Lobe

Temporal lobe specimens were fixed in buffered formalin overnight and sectioned in a coronal plane at 5 mm intervals and at a thickness of 4-μm after routine processing for histology. The sections were stained with Hematoxylin and Eosin, followed by Luxol fast blue, only for cases with an ill-defined gray-white junction. All glass slides were reviewed by a neuropathologist. The histologic features were assessed in white matter at 1 or 2 cm from the temporal lobe pole. In each case, three different sections of the temporal lobe specimens containing a considerable amount of white matter were selected to facilitate the counts of isolated heterotopic neurons (7). Under an optical microscope (Olympus BX50, Olympus Optical Co., Japan), isolated heterotopic neurons counts were obtained in the white matter at greater than 3 mm deep from the gray-white junction and at an objective magnification of 200X. The counts were taken by a neuropathologist, who counted the total number of heterotopic neurons in three different fields (field size of 1 mm^2) per section. Heterotopic neuron numbers are presented as percentages of the total numbers found in nine different fields per case.

The criteria used to determine WCAT included a decreased demarcation of the gray and white matter boundaries, or an increased signal intensity of white matter at the anterior temporal lobe on oblique coronal T2-weighted MR images (7).

Statistics

For VBM analyses, a one way ANOVA (analysis of variance) was used for the concentration analyses of unmodulated gray and white matter images. In addition, an ANCOVA (analysis of covariance) with gray matter volume (GMV) as a covariate was used for the regional volume change analyses using modulated images. To correct for multiple comparisons, the results were corrected using a false discovery rate correction at a significance level of $p < 0.05$. The voxel clusters were corrected with an extent threshold of $k_E > 200$ voxels.

Correlation analyses were performed using SPM2 using a whole brain mask between the heterotopic neuron counts and the GMCs and WMCs. The mean values of significant clusters were extracted from gray and white matter images at an uncorrected significance level of $p < 0.001$, followed by a simple and partial correlation with the control of age at disease onset and disease duration between GMCs or WMCs and the heterotopic neuron counts. Gender distributions were tested using the Pearson Chi-square test. Age, disease duration, and age at disease onset were tested using the two-tailed t-test. Statistical analyses were performed using SPSS version 11.5 (SPSS Inc, Chicago, IL).

Coordinates were defined in accordance with the Montreal Neurological Institute (MNI) coordinate system, and cluster regions were named as described in Duvernoy's atlas (11).

RESULTS

Clinical Data

Age and sex were not different between patients with left mTLE and normal controls. The same is true for right mTLE patients and normal controls. Age at seizure onset and disease duration were not different in the left and right mTLE patient groups, but the frequency of WCATs was significantly higher in the right mTLE group compared to the left mTLE group, and the number of heterotopic neurons of the right mTLE group was greater than that of the left mTLE group (Table 1).

Gray Matter Concentration Analysis

In left mTLE patients, GMCs were reduced in the left hippocampus, bilateral thalami, precentral gyri, superior frontal gyri, cingulate gyri, left supramarginal gyrus, and

Table 1. Demographic Variables in Subjects

	Left			Right		
	Controls	mTLE	*P*	Controls	mTLE	*P*
Number of subject (man:woman)	24 (8:16)	16 (5:11)	0.89*	23 (12:11)	15 (7:8)	0.740*
Age (mean ± SD) (years)	32.2 ± 9.05	32.7 ± 8.47	0.856†	29.8 ± 11.42	28.7 ± 10.59	0.755†
Age of onset (years)	–	18.7 ± 8.55	–	–	15.2 ± 9.96	0.300
Duration of disease (years)	–	13.8 ± 8.77	–	–	13.5 ± 8.68	0.930
Heterotopic neurons§	–	5.46 ± 3.23			7.8 ± 5.86	
(range, subjects)		(2–11, 14/16)	–	–	(2–26, 15/15)	0.060
WCAT	–	25% (4/16)	–	–	60% (9/15)	0.048

Note.— * Pearson Chi-square, † *t* test, ‡ represented in neurons/mm²
mTLE = mesial temporal lobe epilepsy, onset = age of seizure onset, duration = disease duration, SD = standard deviation, WCAT = whiter matter change of anterior temporal lobe in T2-weighted MRI

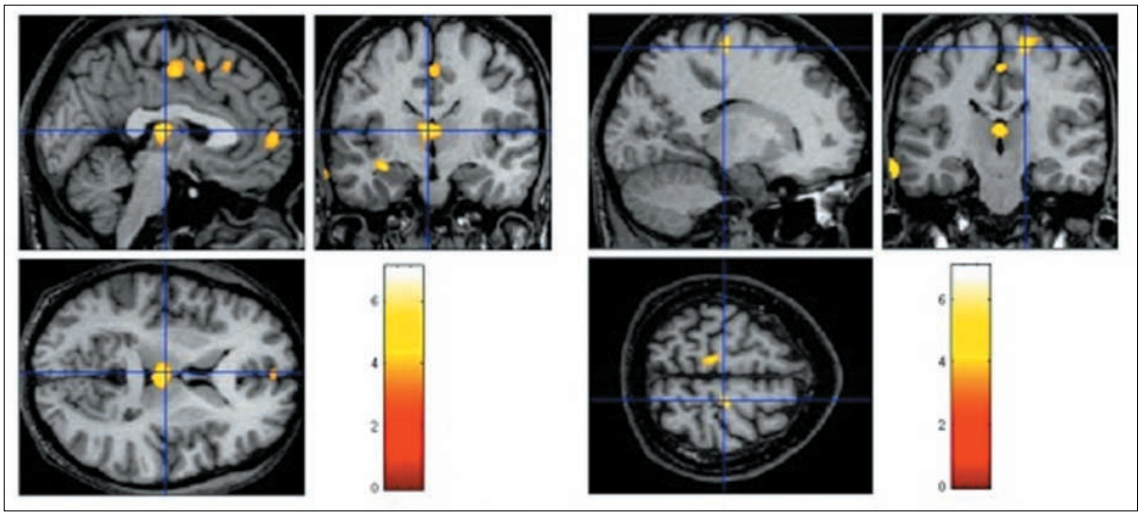

A

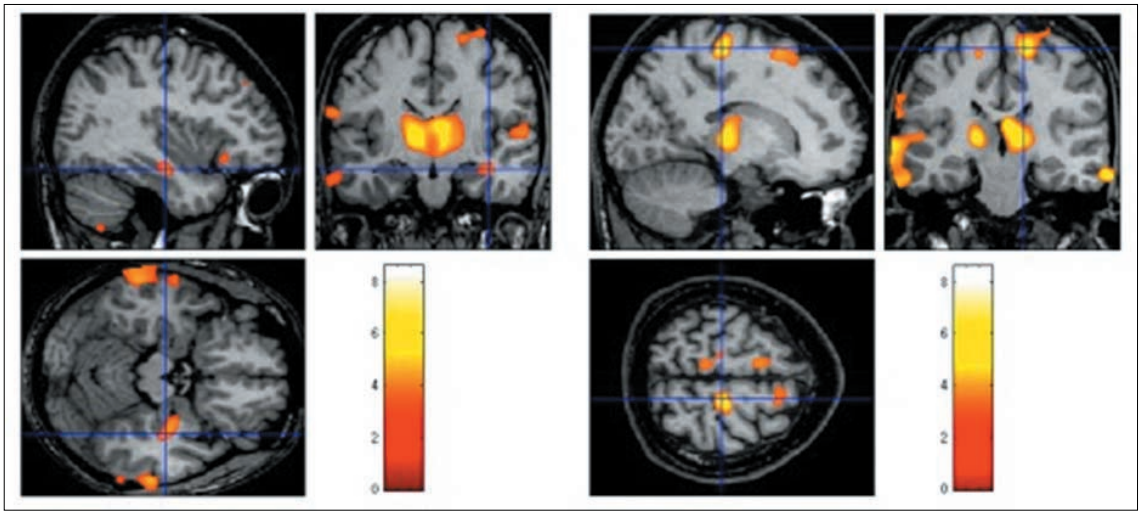

B

Fig. 1. Decreased gray matter concentration in mesial temporal lobe epilepsy. (**A**) shows reduced gray matter concentrations in left hippocampus, bilateral thalami, precentral gyri, superior frontal gyri, and cingulate gyri in left mesial temporal lobe epilepsy patients, whereas (**B**) reveals a gray matter concentration reduction in right hippocampus, thalami, precentral gyri, and frontopolar gyri in right mesial temporal lobe epilepsy patients. These findings were significant at corrected false discovery rate of $p < 0.05$.

cerebellum (Fig. 1A) (Table 2). Regional GMVs in left mTLE were reduced in the bilateral frontopolar gyri, cingulate gyri, caudate nuclei, left thalamus, both hippocampi, left insular gyrus, pons, and cerebellum (Fig. 2A).

In right mTLE patients, GMCs were reduced in the right hippocampus, bilateral thalami, precentral gyri, frontopolar gyri, left inferior frontal gyrus, bilateral superior frontal gyri, superior temporal gyri, middle temporal gyri, and cerebellum (Fig. 1B) (Table 3). Regional GMVs in right mTLE were reduced in the bilateral frontopolar gyri, caudate nuclei, thalami, hippocampi, left orbital gyrus, left superior and middle temporal gyri, and cerebellum (Fig. 2B). There was no increased GMC or volume in both mTLEs.

White Matter Concentration Analysis

In the left mTLE group, WMCs were reduced in the left temporal stem (anterior part), left entorhinal area, both parahippocampal areas, both internal capsules (anterior limb), and in both cingulate gyri (Fig. 3A), whereas the WMCs of the pons and both precentral gyri were increased (Fig. 3B) (Table 4).

In right mTLE group, WMCs were reduced in the right temporal stem (anterior part), right internal capsule (anterior limb), and both the parahippocampal areas, whereas the WMCs increased in the pons, both internal capsules (retrolentiform part), right precentral gyrus, and the left paracentral lobule (Fig. 3C, D).

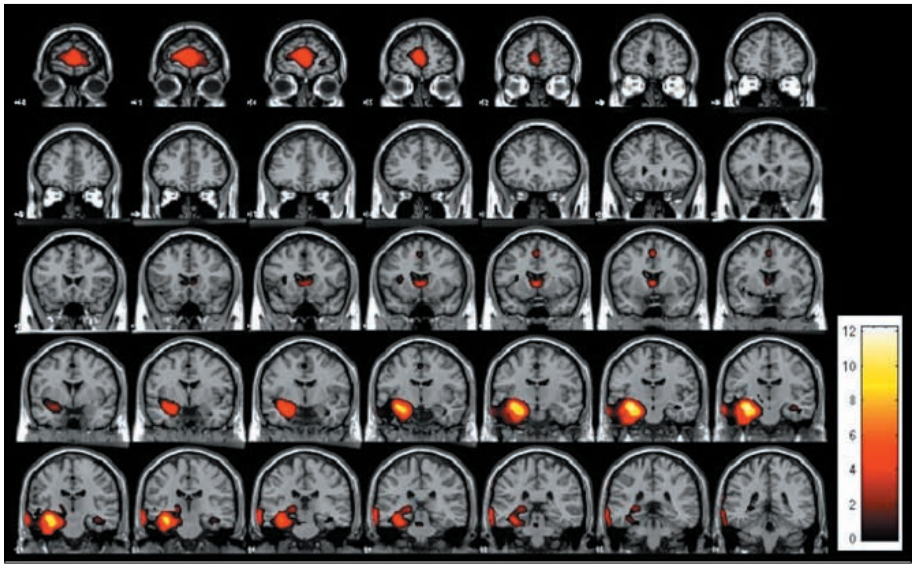

A

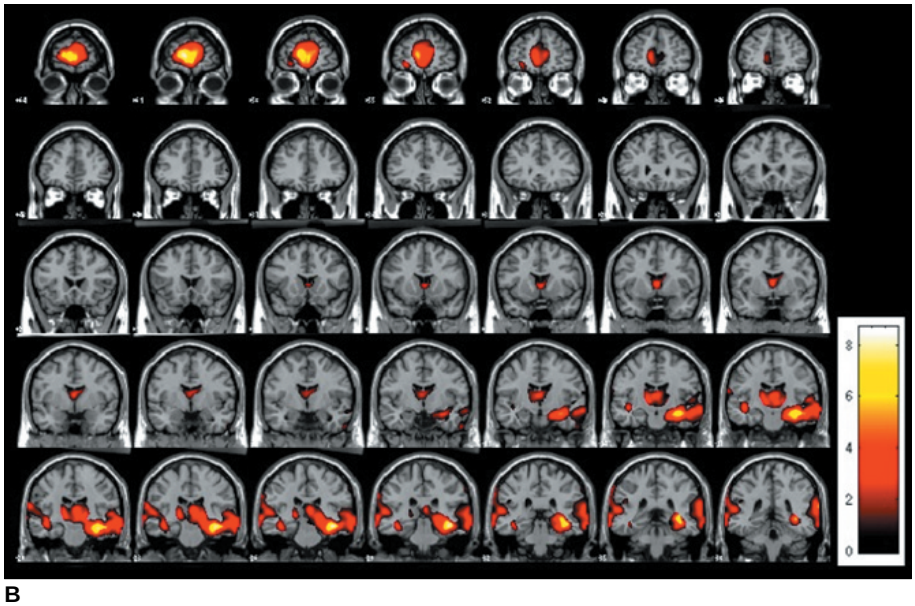

B

Fig. 2. Decreased gray matter volume in mesial temporal lobe epilepsy.
A. MR images show reduced gray matter volumes in bilateral frontopolar gyri, cingulate gyri, caudate nuclei, left thalamus, hippocampi, left insular gyrus, pons, and cerebelli in left mesial temporal lobe epilepsy patients.
B. MR images show gray matter volume reduction in bilateral frontopolar gyri, left orbital gyrus, caudate nuclei, thalami, hippocampi, left superior/middle temporal gyri, and cerebelli in right mesial temporal lobe epilepsy patients. Volume reductions in ipsilateral whole temporal lobes were observed in left and right mesial temporal lobe epilepsy groups. These findings were significant at corrected false discovery rate of $p < 0.05$.

Correlation between Heterotopic Neuron Numbers and Gray, White Matter Concentrations

The WMCs (maximum: 1, minimum: 0) of the anterior temporal stems of the left mTLE patients were found to be negatively correlated with heterotopic neuron counts (x, y, z = −44, −5, −24, voxel level: uncorrected $p = 0.000025$, cluster level: family-wise error [FWE] corrected $p = 0.041$, z = 4.05, $k_E = 912$ voxels). A simple correlation analysis indicated that WMCs and heterotopic neuron counts were negatively correlated ($r = -0.839$, $p = 0.00005$), and a partial correlation analysis (controlling for age at onset and disease duration) confirmed this ($r = -0.861$, $p < 0.001$). Whole brain masks, uncorrected $p < 0.001$, and an extent threshold $k_E > 200$ voxels, were utilized for the correlation analyses (Fig. 4A).

Heterotopic neuron counts were positively correlated with GMCs (maximum: 1, minimum: 0) of the anterior temporal stems of left mTLE patients (x, y, z = −43, −4, −26, voxel level: uncorrected $p = 0.000018$, cluster level: FWE corrected $p = 0.170$, z = 4.13, $k_E = 956$ voxels). A simple correlation analysis between the GMCs and the heterotopic neuron counts showed a strong positive correlation ($r = 0.819$, $p = 0.00005$). Similarly, a partial correlation analysis with a control of age at seizure onset and disease duration also showed a positive correlation ($r = 0.810$, $p < 0.001$) (Fig. 4B). No correlations were found between heterotopic neuron counts and GMCs or WMCs in right mTLE patients.

Table 2. Voxel-Based Morphometry Results of Gray Matter in Left mesial temporal lobe epilepsy Patients

Location	Side	MNI Coordinates (mm)			T	Z	*Corrected *P*	Uncorrected *P*
		x	y	z				
Unmodulated								
Superior frontal gyrus	B	0	26	52	5.05	4.40	0.011	0.000005
Cingulate gyrus	B	1	−11	48	4.52	4.03	0.021	0.00003
Precentral gyrus (superior)	L	−11	−29	62	4.26	3.84	0.028	0.00006
Precentral gyrus (superior)	R	18	−21	62	4.73	4.18	0.017	0.00002
Inferior frontal gyrus	L	−69	−32	39	5.36	4.61	0.007	0.000002
Thalamus	L	−2	−17	9	4.88	4.29	0.013	0.000009
Thalamus	R	1	−18	8	4.88	4.29	0.013	0.000009
Hippocampus	L	−31	−12	−17	4.93	4.36	0.013	0.000007
Supramarginal gyrus	L	−71	−43	17	4.86	4.27	0.014	0.00001
Cerebellum	L	−48	−58	−58	4.89	4.29	0.013	0.000009
Cerebellum	R	50	−60	−52	4.29	3.86	0.029	0.00006
Modulated								
Frontopolar gyri	B	0	60	5	6.64	5.40	< 0.0001	0.00000003
Cingulate gyri	B	0	8	51	4.87	4.28	0.001	0.000009
Caudate nucleus	L	−13	11	14	3.27	3.05	0.026	0.001
Caudate nucleus	R	10	14	8	3.66	3.37	0.012	0.0004
Thalamus	L	−19	−27	0	4.78	4.21	0.001	0.00001
Hippocampus	L	−33	−17	−16	12.21	7.38	< 0.0001	< 0.00000001
Hippocampus	R	40	−19	−18	4.36	3.91	0.003	0.00005
Insular gyrus	L	−30	14	10	3.64	3.36	0.013	0.0004
Middle temporal gyrus	L	−73	−28	−7	6.31	5.21	< 0.001	0.0000001
Supramarginal gyrus	L	−71	−45	19	5.86	4.93	< 0.001	0.0000004
Superior parietal gyrus	L	−14	−69	55	4.29	3.86	0.003	0.00006
Superior parietal gyrus	R	11	−68	58	3.24	3.03	0.025	0.0012
Occipital pole	L	−15	−95	11	3.39	3.15	0.023	0.0008
Pons	L	−1	−28	−25	3.73	3.43	0.011	0.0003
Cerebellum	L	−22	−80	−30	4.44	3.97	0.002	0.00004
Cerebellum	R	24	−80	−30	3.52	3.26	0.016	0.0006
Cerebellum	R	55	−65	−45	3.54	3.28	0.016	0.0005

Note.— * false discovery rate corrected *p*, Extent threshold $k_E > 200$
mTLE = mesial temporal lobe epilepsy, MNI = Montreal Neurologic Institute, B = bilateral, L = left, R = right

DISCUSSION

Clinical Considerations

In this study, we uncovered four significant findings; first, the abnormality of the cortico (precentral gyrus)-thalamo-hippocampal network; second, a large GMV reduction in the anterior frontal lobe; third, a structural abnormality in the pontine area; and fourth, a significant correlation between heterotopic neuron counts and GMC or WMC in the left mTLE patients.

Gray matter concentrations were reduced in the hippocampus, thalamus, precentral gyrus, cerebellum, as well as the wide frontal and temporal areas. Previous studies have reported decreased GMCs (1–3, 12, 13), GMVs (4), GMCs and GMVs (14) in the hippocampus, thalamus, and cerebellum. Our finding of decreased GMC in the precentral gyrus supports a previous study (15). We previously reported that ictal hyperperfusion and interictal hypoperfusion of the cortico-thalamo-hippocampal network in patients with mTLE (9), which may be related to the GMC reduction observed in the precentral gyrus in the present study.

In the GMV analysis with modulated gray matter images, GMVs were also decreased in the caudate nucleus, anterior temporal lobe, and frontopolar gyrus. Moreover, hilar cell densities of the resected hippocampi were found to positively correlate with the regional cerebral glucose metabolic rate in the bilateral thalamus, putamen and

Table 3. Voxel-Based Morphometry Results of Gray Matter in Right mesial temporal lobe epilepsy Patients

Location	Side	MNI Coordinates (mm)			T	Z	*Corrected *P*	Uncorrected *P*
		x	y	z				
Unmodulated								
Frontopolar gyrus	B	0	49	23	3.95	3.60	0.018	0.0002
Superior frontal gyrus	R	14	22	58	3.68	3.39	0.028	0.0004
Superior frontal gyrus	L	−8	−2	55	4.07	3.69	0.015	0.0001
Precentral gyrus (superior)	R	15	−24	63	6.02	5.03	0.001	0.0000003
Precentral gyrus (superior)	L	−8	−35	64	3.64	3.36	0.040	0.0004
Inferior frontal gyrus (posterior)	L	−71	−31	31	4.11	3.72	0.015	0.0001
Thalamus	R	9	−21	4	6.53	5.34	< 0.001	0.00000005
Thalamus	L	−10	−17	3	5.90	4.96	0.001	0.0000004
Hippocampus	R	39	−17	−17	4.27	3.84	0.011	0.00006
Superior temporal gyrus	R	69	−39	17	4.22	3.81	0.012	0.00007
Superior temporal gyrus	L	−63	−34	8	4.13	3.74	0.014	0.00009
Middle temporal gyrus	L	−69	−34	−6	6.95	5.57	< 0.001	0.00000001
Inferior temporal gyrus	R	69	−25	−21	5.55	4.74	0.001	0.000001
Inferior temporal gyrus	L	−66	−27	−23	4.63	4.11	0.006	0.00002
Cerebellum	R	47	−63	−54	4.41	3.95	0.008	0.00004
Cerebellum	L	−42	−59	−56	4.53	4.04	0.007	0.00003
Modulated								
Frontopolar gyri	B	0	63	4	8.19	6.21	< 0.0001	< 0.00000001
Orbital gyrus	L	−27	55	−7	5.00	4.37	0.001	0.000006
Caudate nucleus	R	9	2	17	4.20	3.79	0.003	0.00008
Caudate nucleus	L	−8	7	15	3.00	2.83	0.025	0.002
Thalamus	R	3	−22	12	5.09	4.43	0.001	0.000005
Thalamus	L	−14	−19	2	4.92	4.31	0.001	0.000008
Hippocampus	R	38	−21	−18	8.11	6.17	< 0.0001	< 0.00000001
Hippocampus	L	−40	−27	−15	5.69	4.83	< 0.001	0.0000007
Superior temporal gyrus	L	−58	−32	9	4.38	3.93	0.003	0.00004
Middle temporal gyrus	L	−73	−29	−10	5.52	4.72	< 0.001	0.000001
Superior parietal gyrus	R	13	−68	60	3.57	3.30	0.013	0.0005
Inferior occipital gyrus	R	28	−87	−15	5.16	4.48	0.001	0.000004
Inferior occipital gyrus	L	−25	−87	−13	4.27	3.84	0.004	0.00006
Cerebellum	R	25	−80	−30	3.31	3.09	0.019	0.001
Cerebellum	L	−21	−81	−34	5.52	4.72	< 0.001	0.000001

Note.— * false discovery rate (FDR) corrected *p*, Extent threshold $k_E > 200$
mTLE = mesial temporal lobe epilepsy, MNI = Montreal Neurologic Institute, B = bilateral, L = left, R = right

globus pallidus, and ipsilateral caudate (16). This relationship suggests that hippocampal cell loss causes efferent synaptic activity reductions to the thalamus and basal ganglia, hence decreasing neuronal activity and consequently decreased cerebral glucose metabolism in these structures. Similar to a previous study (17), volume reductions via manual volumetry have been reported in the entorhinal, perirhinal, and temporopolar cortices of drug-refractory mTLE in the present study. The large volume reductions of the anterior frontal lobe in the present study appear to be a new finding. A positive correlation has been reported between hippocampal volume and regional GMVs in the hippocampus, thalamus, and cingulated gyrus, whereas normal controls showed no such correlation (6). Previously, we reported ictal hypoperfusions of the anterior frontal lobe (9, 18). Three mechanisms of ictal hypoperfusion have been suggested, which include a steal phenomenon (19), ictal surround inhibition (20), and regional postictal hypoperfusion during the ictal state due to rapid seizure propagation to other brain regions (9, 21).

The white matter abnormalities in mTLE have been previously reported by VBM and diffusion tensor imaging studies (1, 5, 14, 22). Decreased WMC and white matter volume (WMV) has been reported in the ipsilateral parahippocampal gyrus as well as in the contra-lateral internal capsule (14), and decreased WMC in the ipsilateral temporopolar, temporal stem, entorhinal, and perirhinal areas (1). In addition, reduced WMV were also observed in ipsilateral temporopolar, temporal stem, corpus callosum, and anterior frontal areas (5). Decreased fractional anisotropy has been reported in the entorhinal cortex, corpus callosum, and in the anterior limb of the internal capsule, indicating diffuse white matter loss in the limbic system (22). The results of the present study support these findings.

Table 4. Voxel-Based Morphometry Results of White Matter in mTLE Patients

Location	Change	Side	MNI Coordinates (mm)			T	Z	*Corrected *P*	Uncorrected *P*
			x	y	z				
Left mTLE									
Temporal stem (anterior part)	Decreased	L	−42	4	−31	4.77	4.08	0.03	0.000022
Entorhinal area	Decreased	R	31	0	−30	4.77	4.08	0.03	0.000022
Parahippocampal area	Decreased	L	−24	−23	−15	9.62	6.45	0.03	< 0.000000001
Parahippocampal area	Decreased	R	24	−19	−15	6.13	4.90	0.03	0.0000005
Internal capsule (anterior limb)	Decreased	L	−8	5	4	5.64	4.62	0.03	0.000002
Internal capsule (anterior limb)	Decreased	L	−15	15	−9	5.57	4.58	0.03	0.0000023
Internal capsule (anterior limb)	Decreased	R	8	4	7	4.71	4.04	0.03	0.000027
Internal capsule (anterior limb)	Decreased	R	16	19	−8	5.07	4.27	0.03	0.0000097
Cingulate gyri	Decreased	B	0	−4	33	5.22	4.37	0.03	0.0000062
Middle frontal gyrus	Decreased	R	30	42	10	5.01	4.24	0.03	0.000011
Middle temporal gyrus	Decreased	R	51	−34	−4	5.01	4.24	0.03	0.000011
Superior temporal gyrus	Decreased	R	47	−5	−12	4.82	4.11	0.03	0.00002
Pons	Increased	B	0	−17	−43	5.50	4.54	0.03	0.0000028
Precentral gyrus	Increased	R	17	−20	67	6.63	5.17	0.03	0.00000012
Precentral gyrus	Increased	L	−15	−28	63	5.18	4.34	0.03	0.0000071
Right mTLE									
Temporal stem (anterior part)	Decreased	R	34	0	−32	4.62	3.97	0.036	0.000037
Parahippocampal area	Decreased	R	23	−20	−15	4.93	4.17	0.036	0.000016
Parahippocampal area	Decreased	L	−23	−20	−16	4.62	3.96	0.036	0.000037
Internal capsule (anterior limb)	Decreased	R	9	4	8	7.31	5.46	0.036	0.000000024
Internal capsule (anterior limb)	Decreased	R	11	18	−7	5.20	4.34	0.036	0.0000072
Middle frontal gyrus	Decreased	R	28	42	10	4.20	3.68	0.036	0.00012
Pons	Increased	B	0	−30	−53	4.28	3.73	0.068	0.00009
Internal capsule (retrolentiform part)	Increased	L	−14	−24	4	6.00	4.80	0.068	0.0000008
Internal capsule (retrolentiform part)	Increased	R	14	−22	1	4.50	3.89	0.068	0.00005
Precentral gyrus	Increased	R	16	−24	70	9.96	6.52	0.068	< 0.000000001
Paracental lobule	Increased	L	−20	−40	53	4.78	4.07	0.068	0.000024

Note.— * false discovery rate corrected *p*, Extent threshold $k_E > 200$
mTLE = mesial temporal lobe epilepsy, MNI = Montreal Neurologic Institute, B = bilateral, L = left, R = right

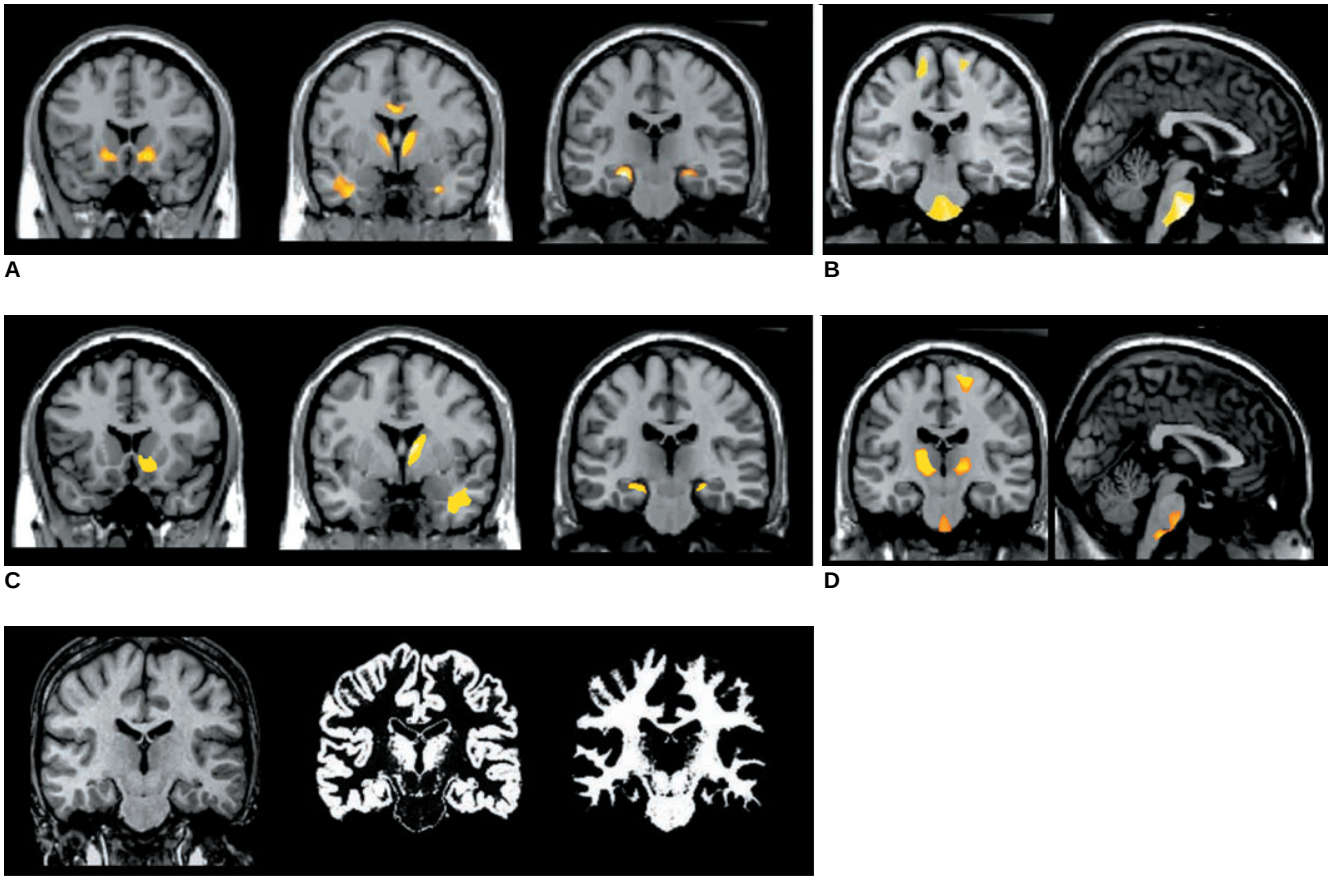

Fig. 3. White matter concentration changes in mesial temporal lobe epilepsy patients. White matter concentrations reduced in internal capsules, temporal stem, and parahippocampal regions in left (**A**) and right (**C**) mesial temporal lobe epilepsy patients, whereas white matter concentrations increased in precentral gyri, pons, and internal capsules in left (**B**) and right (**D**) mesial temporal lobe epilepsy patients. Pons (arrow) was partitioned into white matter image using SPM2 segmentation (**E**). These findings were significant at uncorrected $p < 0.001$.

A previous study reported WMC reduction (1) and WMV reduction (5) in the ipsilateral temporopolar region or temporal stem in mTLE patients. The authors presumed that a cause of WMC reduction may be the secondary damage from repetitive seizure propagations or the deafferentation from GMV reduction of ipsilateral temporal lobes. However, we showed that the WMC in the ipsilateral temporopolar region is negatively correlated with the number of heterotopic neurons in the white matter of the anterior temporal lobe in the left mTLE group (Fig. 4), but not in the right mTLE group. We also previously reported heterotopic neurons in the ipsilateral anterior temporal stem from histologic and ictal rCBF hyperperfusion in the temporal stem of mTLE patients (9). It is unclear why there was no significant correlation between GMC and the heterotopic neuron number of the anterior temporal stem in the right mTLE. The significantly higher frequency of white matter signal changes on T2-weighted MRI and the large number of heterotopic neurons in right mTLE than in left mTLE patients could suggest some differences in histologic changes or pathogenesis between the left and right mTLE patients. The right hippocampus has been reported to be larger than the left hippocampus in the normal population (23, 24), and a previous study showed that right mTLE showed more frequent propagations of ictal discharges to the contralateral hemisphere (9). Thus, more studies are needed for further clarification of the relationship between heterotopic neurons and GMC or WMC in anterior temporal stem.

A previous study showed the occurrence of other histologic changes in temporal lobe white matter; for example, diffuse glial cell proliferation, perivascular space enlargement, neuronal heterotopia, astrocytic gliosis, increased numbers of corpora amylacea, and increased oligodendroglial cell clusters (7). It has been suggested that WCAT may be a nonspecific reactive change to seizure discharges (25), or a chronic excitotoxic injury caused by seizure activity (26).

Complex partial seizures originating from the temporal lobe frequently propagate to the brainstem and thalamus,

and are related to loss of consciousness during seizures (27, 28). The abnormality of the pontine area in the present study could be related with seizure propagations in the mTLE.

Methodological Considerations

In spatial normalization, there are two options for the 'unmodulation' process for brain tissue concentration and 'modulation' process for brain tissue volume change. In order to preserve the total amount of signal in the images, the areas expanded during warping are correspondingly reduced in intensity, and areas contracted during warping are increased in intensity. This 'modulation' process multiplies tissue voxel values by the Jacobian determinants, and yields the determinant of the deformation parameters obtained from spatial normalization. So the use of the 'modulation' process could reflect the regional volume change. The 'unmodulated' images preserve its own signal intensities regardless of the expansion or contraction during warping. Hence, the VBM results using 'unmodulated' images could reflect the GMCs or WMCs (10, 29, 30).

In the present study, gray matter images were normalized to our study specific gray matter template, and the normalization parameters of the gray matter images were applied to the white matter images. There may be debate as to the choice of gray or white matter template for the white matter analysis in the VBM study. The problem is that white matter (WM) is characterized by large uniform areas with only minor signal contrast regardless of the

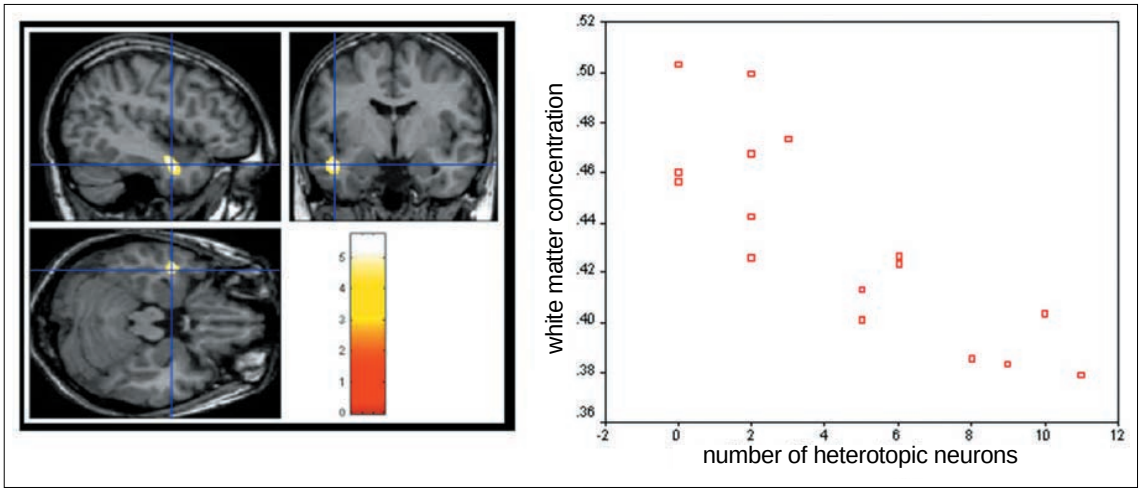

A

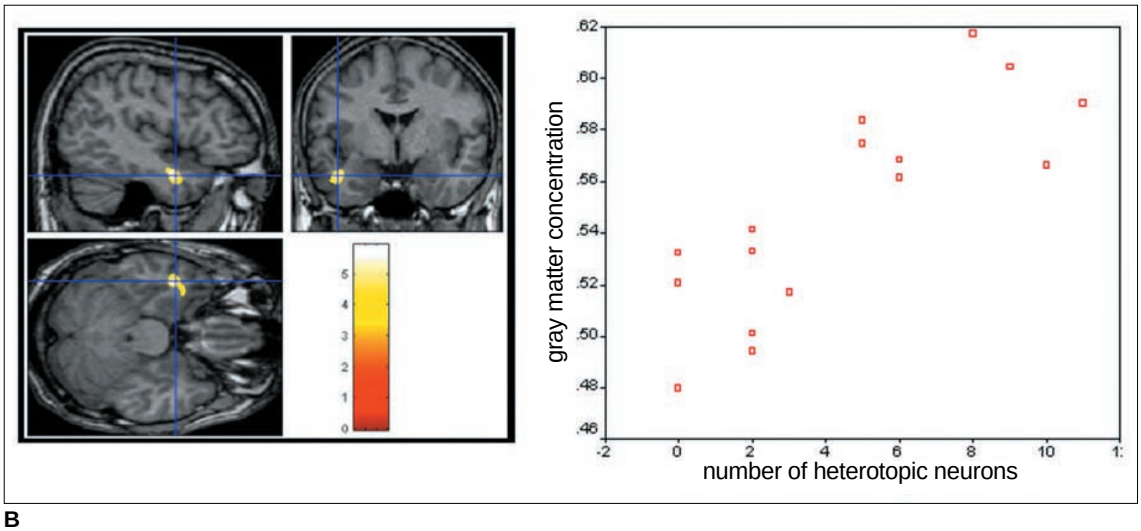

B

Fig. 4. Correlation between gray and white matter concentrations and heterotopic neuron counts in left mesial temporal lobe epilepsy. Negative correlation (r = −0.839, p = 0.00005) was found between white matter concentration and heterotopic neuron count in left anterior temporal lobe (**A**), whereas a positive correlation (r = 0.819, p = 0.00005) was observed between gray matter concentration and heterotopic neuron count in left anterior temporal lobe (**B**). Whole brain mask with uncorrected $p < 0.001$, and extent threshold of $k_E >$ 200 voxels were applied for statistical parametric mapping analysis.

large or small WM area. In contrast, gray matter (GM) provides much more detail because the GM band is only several millimeters thin. The registration usually relies on image intensity gradients, which can be found for WM only at the borders. Thus, the quality of WM registration is inferior to GM registration. The voxel-based morphometry approach is usually based on GM registration because of these reasons. We have tried both approaches and got the superior results for WM registration using the gray matter normalization parameters supporting this notion.

Increased WMCs in the precentral gyrus and internal capsule close to the thalamus appear to be attributed to an expansion effect of white matter during spatial normalization. Because the GMCs and GMVs were reduced in the precentral gyrus and thalamus, white matter might have expanded to compensate for gray matter loss during spatial normalization. This is a false positive finding coming from a methodological problem; hence, the researcher should be careful in interpreting the results of their VBM studies.

Despite the subcortical nuclei present in the pons, the pontine area was classified as a white matter image due to low intensity in the T1 MR images in the present study (Fig. 3E). The intensity of one voxel is composed of gray matter, white matter, and CSF intensities (the intensity of gray matter + white matter + CSF =1). If the neuronal density in the pons is low, the pontine area may appear to have higher WMC in T1 MR images. Thus, increased WMC in the pontine area may biologically reflect reduced neuronal density.

In conclusion, the present study demonstrates an abnormality of the hippocampal-thalamo-cortical network, GMV reduction in the anterior frontal lobe, a structural abnormality in the pontine area, and correlations between heterotopic neuron counts and the GMC and WMC in the white matter of the left anterior temporal lobe. However, future investigations should explore in more detail the neuronal correlation with the GMCs in the anterior temporal white matter.

References

1. Bernasconi N, Duchesne S, Janke A, Lerch J, Collins DL, Bernasconi A. Whole-brain voxel-based statistical analysis of gray matter and white matter in temporal lobe epilepsy. *Neuroimage* 2004;23:717-723
2. Bonilha L, Rorden C, Castellano G, Cendes F, Li LM. Voxel-based morphometry of the thalamus in patients with refractory medial temporal lobe epilepsy. *Neuroimage* 2005;25:1016-1021
3. Bonilha L, Rorden C, Castellano G, Pereira F, Rio PA, Cendes F, et al. Voxel-based morphometry reveals gray matter network atrophy in refractory medial temporal lobe epilepsy. *Arch Neurol* 2004;61:1379-1384
4. Wehner T, Luders H. Role of neuroimaging in the presurgical evaluation of epilepsy. *J Clin Neurol* 2008;4:1-16
5. McMillan AB, Hermann BP, Johnson SC, Hansen RR, Seidenberg M, Meyerand ME. Voxel-based morphometry of unilateral temporal lobe epilepsy reveals abnormalities in cerebral white matter. *Neuroimage* 2004;23:167-174
6. Duzel E, Schiltz K, Solbach T, Peschel T, Baldeweg T, Kaufmann J, et al. Hippocampal atrophy in temporal lobe epilepsy is correlated with limbic systems atrophy. *J Neurol* 2006;253:294-300
7. Choi D, Na DG, Byun HS, Suh YL, Kim SE, Ro DW, et al. White-matter change in mesial temporal sclerosis: correlation of MRI with PET, pathology, and clinical features. *Epilepsia* 1999;40:1634-1641
8. Hammers A, Koepp MJ, Hurlemann R, Thom M, Richardson MP, Brooks DJ, et al. Abnormalities of grey and white matter [11C] flumazenil binding in temporal lobe epilepsy with normal MRI. *Brain* 2002;125:2257-2271
9. Tae WS, Joo EY, Kim JH, Han SJ, Suh YL, Kim BT, et al. Cerebral perfusion changes in mesial temporal lobe epilepsy: SPM analysis of ictal and interictal SPECT. *Neuroimage* 2005;24:101-110
10. Good CD, Johnsrude IS, Ashburner J, Henson RN, Friston KJ, Frackowiak RS. A voxel-based morphometric study of ageing in 465 normal adult human brains. *Neuroimage* 2001;14:21-36
11. Duvernoy HM. *The human brain: surface, three-dimensional sectional anatomy, and MRI, and blood supply*. New York: Springer-Verlag, 1999
12. Keller SS, Mackay CE, Barrick TR, Wieshmann UC, Howard MA, Roberts N. Voxel-based morphometric comparison of hippocampal and extrahippocampal abnormalities in patients with left and right hippocampal atrophy. *Neuroimage* 2002;16:23-31
13. Keller SS, Wieshmann UC, Mackay CE, Denby CE, Webb J, Roberts N. Voxel based morphometry of grey matter abnormalities in patients with medically intractable temporal lobe epilepsy: effects of side of seizure onset and epilepsy duration. *J Neurol Neurosurg Psychiatry* 2002;73:648-655
14. Mueller SG, Laxer KD, Cashdollar N, Buckley S, Paul C, Weiner MW. Voxel-based optimized morphometry (VBM) of gray and white matter in temporal lobe epilepsy (TLE) with and without mesial temporal sclerosis. *Epilepsia* 2006;47:900-907
15. Keller SS, Cresswell P, Denby C, Wieshmann U, Eldridge P, Baker G, et al. Persistent seizures following left temporal lobe surgery are associated with posterior and bilateral structural and functional brain abnormalities. *Epilepsy Res* 2007;74:131-139
16. Dlugos DJ, Jaggi J, O'Connor WM, Ding XS, Reivich M, O'Connor MJ, et al. Hippocampal cell density and subcortical metabolism in temporal lobe epilepsy. *Epilepsia* 1999;40:408-413
17. Jutila L, Ylinen A, Partanen K, Alafuzoff I, Mervaala E, Partanen J, et al. MR volumetry of the entorhinal, perirhinal, and temporopolar cortices in drug-refractory temporal lobe epilepsy. *AJNR Am J Neuroradiol* 2001;22:1490-1501
18. Lee HW, Hong SB, Tae WS. Opposite ictal perfusion patterns of subtracted SPECT. Hyperperfusion and hypoperfusion. *Brain* 2000;123:2150-2159
19. Rabinowicz AL, Salas E, Beserra F, Leiguarda RC, Vazquez SE. Changes in regional cerebral blood flow beyond the temporal lobe in unilateral temporal lobe epilepsy. *Epilepsia* 1997;38:1011-1014
20. Prince DA, Wilder BJ. Control mechanisms in cortical epileptogenic foci. "Surround" inhibition. *Arch Neurol* 1967;16:194-202

21. Lieb JP, Dasheiff RM, Engel J Jr. Role of the frontal lobes in the propagation of mesial temporal lobe seizures. *Epilepsia* 1991;32:822-837
22. Arfanakis K, Hermann BP, Rogers BP, Carew JD, Seidenberg M, Meyerand ME. Diffusion tensor MRI in temporal lobe epilepsy. *Magn Reson Imaging* 2002;20:511-519
23. Jack CR Jr, Twomey CK, Zinsmeister AR, Sharbrough FW, Petersen RC, Cascino GD. Anterior temporal lobes and hippocampal formations: normative volumetric measurements from MR images in young adults. *Radiology* 1998;172:549-554
24. Jack CR Jr. MRI-based hippocampal volume measurements in epilepsy. *Epilepsia* 1994;35:S21-S29
25. Kim JH, Murdoch GH, Hufnagel TJ, Shen MY, Harrington WN, Spencer DD. White matter changes in intractable temporal lobe epilepsy [abstract]. *Epilepsia* 1990;31:630
26. Chung MH, Horoupian DS. Corpora amylacea: a marker for mesial temporal sclerosis. *J Neuropathol Exp Neurol* 1996;55:403-408
27. Dreifuss S, Vingerhoets FJ, Lazeyras F, Andino SG, Spinelli L, Delavelle J, et al. Volumetric measurements of subcortical nuclei in patients with temporal lobe epilepsy. *Neurology* 2001;57:1636-1641
28. Lee KH, Meador KJ, Park YD, King DW, Murro AM, Pillai JJ, et al. Pathophysiology of altered consciousness during seizures: subtraction SPECT study. *Neurology* 2002;59:841-846
29. Ashburner J, Friston KJ. Nonlinear spatial normalization using basis functions. *Hum Brain Mapp* 1999;7:254-266
30. Keller SS, Wilke M, Wieshmann UC, Sluming VA, Roberts N. Comparison of standard and optimized voxel-based morphometry for analysis of brain changes associated with temporal lobe epilepsy. *Neuroimage* 2004;23:860-868